A LETTERS JOURNAL EXPLORING THE FRONTIERS OF PHYSICS

January 2020

EPL, **129** (2020) 27004
doi: 10.1209/0295-5075/129/27004

www.epljournal.org

The electric-field–induced "zero-degree domain walls" in ferromagnets

Filuza A. Maksutova[1,2], Rostislav V. Solonetskiy[3], Robert M. Vakhitov[2] and Alexander P. Pyatakov[1(a)]

[1] *Physics Department, M.V. Lomonosov Moscow State University - Leninskie gori, MSU, 119991, Moscow, Russia*
[2] *Bashkir State University - 32, Z. Validy Str., 450076, Ufa, Russia*
[3] *Ufa State Aviation Technical University - 12, K. Marx Str. 450008, Ufa, Russia*

received 30 September 2019; accepted in final form 29 January 2020
published online 24 February 2020

PACS 75.85.+t – Magnetoelectric effects, multiferroics
PACS 77.55.Nv – Multiferroic/magnetoelectric films

Abstract – The internal structure of electric-field–induced magnetic topological defects in dielectric magnetic film with inhomogeneous magnetoelectric effect is considered. It is shown that this "zero-degree domain wall" has a complex internal structure with the sense of magnetization rotation and corresponding electric polarity changing twice across the wall. The two possible solutions corresponding to 0° domain walls (the pure cycloidal domain wall and the mixed one) as well as their energies are analyzed. It is shown that the 0° domain wall is a transitional state between the homogeneously magnetized media and the electric-field–induced magnetic domain. The critical field of the domain nucleation obtained from this model is within the range of experimental values of several MV/cm.

Introduction. – The concepts of coupling between magnetism and ferroelectricity in multiferroics and magnetoelectric media have evolved dramatically since the beginning of the century [1–3]. One of the new trends in multiferroics studies is the magnetoelectricity localized on domain walls, magnetic vortices, skyrmions and other magnetic topological defects [4–8].

Electric-field–induced effects have recently been shown to play an important role in micromagnetism: both in multiferroic media [9] and in magnets with central symmetry [10]. Various magnetoelectric phenomena were observed on micromagnetic structures in iron garnet films: the domain wall motion driven by electric field [11–13] the inverse effect of magnetic switching of the domain wall electric polarity [14], direct detection of the electric field associated with magnetic domain wall [15], the electric-field–induced Bloch line displacement and domain wall broadening [16,17], and quite recently the magnetic bubble domain generation in single domain state [18,19].

About a decade ago I. E. Dzyaloshinskii in the seminal paper *Magnetoelectricity in ferromagnets* [10] predicted that a topological defect, *e.g.*, a Néel-type domain wall, can be generated in a single domain state by the electric field exceeding the certain threshold value. Due to the boundary condition (the newborn magnetic topological defect is surrounded by the initial single domain state) the integral angle of the magnetization rotation in this type of the structure should be zero. This *zero-degree domain wall* (0°-DW) can be considered as an initial state of bubble domain nucleation observed in experiments [18–21], thus the magnetization distribution in it should be studied in more detail.

The relation between electric field and inhomogeneous magnetization distribution in ferromagnet is described by the Lifshitz-type invariant term linear with respect to the spatial derivatives of the magnetic order parameter $\mathbf{m}$ [22–26]:

$$W_{ME} = M_S^2(\mathbf{E}\cdot\{b_1\mathbf{m}\,\mathrm{div}\,\mathbf{m} + b_2[\mathbf{m}\times\mathrm{rot}\,\mathbf{m}]\}), \qquad (1)$$

where M_s is the saturation magnetization, $\mathbf{E}$ is the strength of the electric field, b_1, b_2 are the constants of inhomogeneous magnetoelectric interaction [27], $\mathbf{m} = \mathbf{M}/M_s$ is the unit magnetization vector. This type of magnetoelectric interaction is the origin of spin cycloid in multiferroics [28] as well as magnetically induced ferroelectricity in spiral magnets [24,29].

In this letter we show that the micromagnetic structure of the electric-field–induced 0° domain wall differs from

(a) E-mail: pyatakov@physics.msu.ru

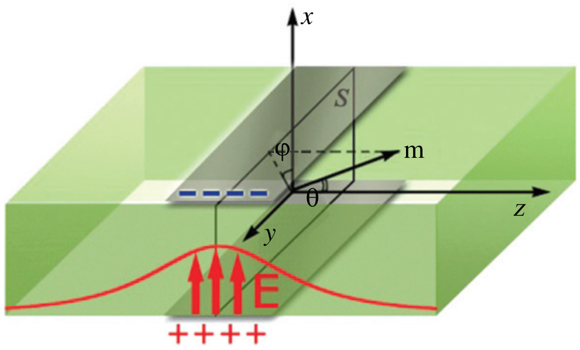

Fig. 1: The geometry of the problem. E is the electric field of the electrode, $\mathbf{m}$ is the unit magnetization vector in the film.

the conventional one and implies reversals of the sense of magnetization rotation across the domain wall. It has a complex structure comprising the central part of the domain wall ("nucleus") and two "tails" that have the opposite sense of magnetization rotation with respect to the nucleus.

The model. – Let us consider a film of uniaxial ferromagnetic dielectric material with ME interaction described by eq. (1) placed in a non-uniform electric field perpendicular to the film surface. The geometry of the problem is shown in fig. 1: the polar axis Oz is oriented along the direction of magnetization modulation, the Ox-axis is along normal to the film is taken to be parallel to the crystal symmetry axis.

We assume that the non-uniform distribution of magnetization is induced by the non-uniform electric field and proceed by considering free energy represented in the form

$$\begin{aligned} W = \int_{-\infty}^{\infty} \Bigg\{ & A\left[\left(\frac{\mathrm{d}\theta}{\mathrm{d}z}\right)^2 + \sin^2\theta\left(\frac{\mathrm{d}\varphi}{\mathrm{d}z}\right)^2\right] \\ & + K_u(\sin^2\varphi\sin^2\theta + \cos^2\theta) \\ & + M_s^2 E\left[-(b_1\sin^2\theta + b_2\cos^2\theta)\cos\varphi\frac{\mathrm{d}\theta}{\mathrm{d}z}\right. \\ & \left. + b_2\sin\varphi\sin\theta\cos\theta\frac{\mathrm{d}\varphi}{\mathrm{d}z}\right] + 2\pi M_s^2\cos^2\theta\Bigg\}\,\mathrm{d}z, \quad (2) \end{aligned}$$

where θ, φ are, respectively, the polar and azimuthal angles of the unit magnetization vector $\mathbf{m}$, A is the exchange stiffness constant, K_u is the constant of uniaxial magnetic anisotropy. Hereinafter we suppose that the non-uniform electric field, whose strength is determined by the law

$$E_x = E_o/\mathrm{ch}(z/L), \quad (3)$$

acts in the restricted area, where L is the width of the area subjected to non-uniform electric field, E_o is the magnitude of the electric-field strength in the center of the stripe electrode $y = 0$.

The equilibrium distribution of $\theta(z)$, $\varphi(z)$ are determined by solving a set of Euler-Lagrange equations minimizing the energy functional (1)

$$\begin{aligned} & \mathrm{d}(\sin^2\theta\mathrm{d}\varphi/\mathrm{d}\xi)/\mathrm{d}\xi - \sin\varphi\cos\varphi\sin^2\theta \\ & -(\lambda_1+\lambda_2)f(\xi)\sin\varphi\sin^2\theta\mathrm{d}\theta/\mathrm{d}\xi \\ & +\lambda_2\sin\varphi\sin\theta\cos\theta\mathrm{d}f/\mathrm{d}\xi = 0, \\ & \mathrm{d}^2\theta/\mathrm{d}\xi^2 + \sin\theta\cos\theta[\cos^2\theta - (\mathrm{d}\varphi/\mathrm{d}\xi)^2] \\ & +(\lambda_1+\lambda_2)f(\xi)\sin\varphi\sin^2\theta\mathrm{d}\varphi/\mathrm{d}\xi - (\lambda_1\sin^2\theta+\lambda_2\cos^2\theta) \\ & \times\cos\varphi\mathrm{d}f/\mathrm{d}\xi + Q^{-1}\sin\theta\cos\theta = 0, \quad (4) \end{aligned}$$

where $\varepsilon_i = E_o/E_i$, $E_i = 2K_u\Delta_0/M_s^2 b_i$, $i = 1, 2$, $\zeta = z/\Delta_0$, $l = L/\Delta_0$, $\Delta_0 = \sqrt{A/K_u}$, $f(\zeta) = \mathrm{ch}^{-1}(\zeta/l)$.

Here ε, E_i are the dimensionless and the characteristic fields, respectively. $Q = K_u/2\pi M_s^2$ is the quality factor.

Depending on the relation between the constants of magnetic anisotropy, the quality factor, the strength of electric field and the length of electric-field non-uniformity, various spatially modulated structures can be realized in the system. Let us consider the high-symmetry case of isotropic spin flexo-electricity: $b_1 = b_2 = b$. The quality factor $Q = 3$ is close to the value in the experiments [11,14,18].

The analysis of eqs. (4) with single domain state boundary conditions shows that there are two solutions corresponding to the zero-degree domain wall. The magnetization rotation in the electric-field–induced inhomogeneity does not evolve according to the classic Bloch scenario, it is rather the quasi-Bloch–type [30] or pure Néel one.

The quasi-Bloch domain wall has a significant component of the magnetization m_z along the modulation direction (fig. 2), that, according to eq. (1), corresponds to the nonzero electric polarization $P(z) = -\partial W_{ME}/\partial E$. In accordance to eq. (1) the reversal of the sense of magnetization rotation results in the alternating electric polarization: the nucleus of the domain wall with the largest spatial derivative of magnetization is characterized by the maximum of electric polarization while the two tails surrounding the nucleus correspond to the minima with polarization of opposite sign. The normalized dependence of polarization on the dimensionless coordinate, $p(\zeta) = P(\zeta)\Delta_0/(M_s^2 b)$, is shown in the right inset of fig. 2.

Another solution of eqs. (4) corresponding to a 0°-domain wall is a pure Néel-type one (fig. 3): $\varphi = 0$, *i.e.*, magnetization rotates in the Oxz-plane (fig. 1). As in the previous case of quasi-Bloch wall, the Néel 0°-DW has the antisymmetric coordinate dependence $\theta = \theta(z)$ with the extrema growing with the external electric field E_0 growth. The corresponding electric polarization of the domain wall $p(\zeta)$ is the alternating function of the coordinate making the electrical triple layer (fig. 3). The bound surface charge density increases with increasing the electric field E_0 while the electric charge integrated over the domain wall width remains zero which guarantees self-screening of the triple layer. The positions of the surface charge density maxima do not change with increasing the electric field E_0 and depend on the width L of the stripe electrode.

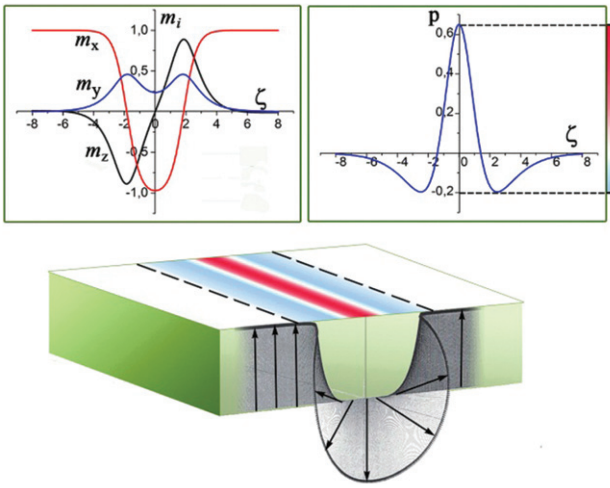

Fig. 2: The magnetization distribution of the quasi-Bloch 0°-DW structure (shown with arrows) and the surface electric charges associated with it (shown with red/blue contrast). The electrode edges are shown with dashed line (the electrode semi-width parameter $l = 5$). Corresponding graphs of the unit magnetization components and dimensionless electric polarization are presented in the insets.

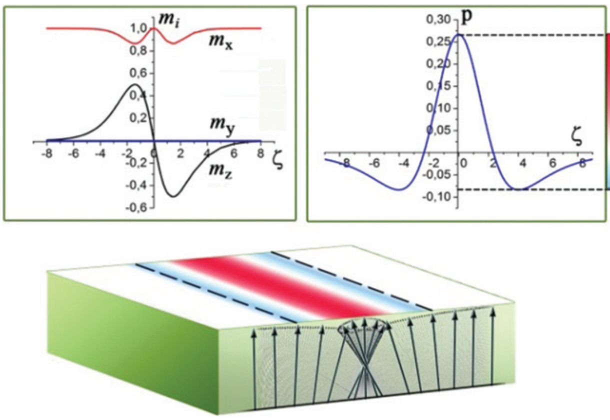

Fig. 3: The magnetization distribution of the Néel-type 0°-DW structure (shown with arrows) and the surface electric charges associated with it (shown with red/blue contrast). The electrode edges are shown with the dashed line (the electrode semi-width parameter $l = 5$). Corresponding graphs are shown in the insets.

Discussion. – The zero-degree magnetic topological defects frequently encountered in magnetic dynamics [31] can also be found as the solution of certain static problems of micromagnetism. These are the micromagnetic structures formed in the vicinity of the I-order spin-orientation phase transitions [32] and the ones hosted by the potential well-type defects: the 0°-DW [33] and the skyrmion-type magnetic vortices [34,35].

The stability of skyrmions and spin cycloids in chiral magnets is provided by the Dzyaloshinskii-Moriya interaction [36,37]. Taking into account that the flexomagnetoelectric term described by eq. (1) can be

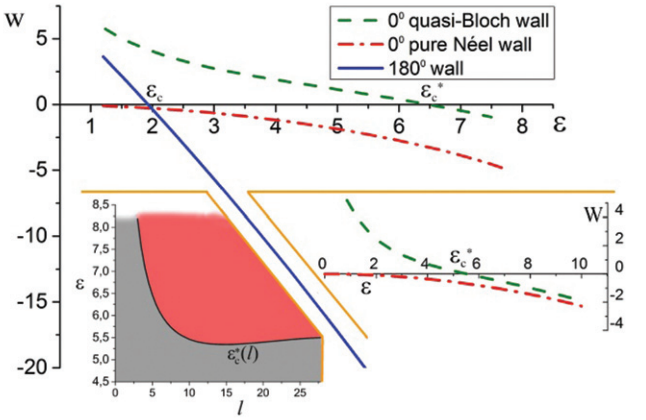

Fig. 4: The dependence of the dimensionless energy w of the micromagnetic structures of various topologies on the reduced field ε with the following parameter values: $l = 5$, $Q = 3$. The solid line corresponds to double 180°-DW, the dashed one corresponds to quasi-Bloch 0°-DW, and the dash-dotted one to the Néel 0°-DW. The phase diagram of the 0°-DW state is shown in the left inset (the red region above the line $\mathcal{E}_c^*(l)$ corresponds to the 0° quasi-Bloch DW, the gray region below the line is the homogenous single domain state). In the right inset the curves for Néel and quasi-Bloch DWs corresponding to $l = 25$ are shown.

derived from the microscopic Dzyaloshinskii-Moria interaction [38], the appearance of the 0°-DW seems natural. In this context the inhomogeneous electric field provided by the stripe electrode can be considered as a potential well-type defect. However the specific feature of the 0°-DW described by eqs. (4) is the nonzero Néel component of the magnetization while the potential well defects previously considered in [33] support the pure Bloch-type 0°-DW state.

The dependences of the DW surface energy on the electric field corresponding to various types of solutions of eqs. (4) are presented in fig. 4. The dimensionless energy w is normalized on the product of anisotropy constant and domain width parameter: $w = W/(K_u\Delta_0)$ (fig. 1).

The zero energy level corresponds to the homogeneous magnetization distribution. The dependence of the double 180° domain wall transforming in electric field from zero-field Bloch state to the Néel one is also shown. It can be seen that in the low-field region the generation of Néel-type 0°-DW defect is energetically favorable. Then at critical field $\mathcal{E}_c$ the double 180° Néel wall becomes energetically preferable, which means nucleation of the new domain with downward magnetization direction. Taking into account the experimental parameters from [11,14,18]: $\Delta_0 = 100\,\text{nm}$, $K_u = 10^3\,\text{erg/cm}^3$, $M_s^2 b_i = 10^{-6}\,\text{CGS}$, the dimensionless value of the critical field $\mathcal{E}_c = 2$ corresponds to electric field $\sim$10 MV/cm that is in agreement with the experimental situation of 1 kV voltage applied to the μm-sized tip electrode [19].

It is interesting to compare the energies of two types 0°-DW: in the gradient field of the stripe electrode the

Néel-type domain wall has lower energy than the quasi-Bloch one while at the homogeneous electric field limit ($l \to \infty$) the energy dependences of two types of 0°-DWs tend to the same asymptotic curve at high electric field values (the right inset of fig. 4). It is reasonable, since the Néel-type domain wall has zero integral charge: the energy of its Coulomb interaction with the electrode is minimized only when the nucleus (with energetically favorable direction of electric polarization) is localized in the region of the maximum strength of the electric field while the negatively polarized tails are expelled to the low electric field region.

Though quasi-Bloch 0°-DW seems to lose the energy competition, it is of interest as one-dimensional analogue of skyrmion. Furthermore, the structural hole-like defects preventing nucleation of the Néel-type domain wall for magnetostatic reasons can support the formation of quasi-Bloch 0°-DW. The phase diagram corresponding to 0°-DW existence area in the coordinates "strength of the field ε and the semi-width of the electrode l" is presented in the left inset of fig. 4).

Conclusion. – Thus in contrast to the originally considered 180°-degree Néel domain wall [10] in this paper we propose the new electric-field–induced 0°-degree structure with the sense of magnetization rotation changing twice across the domain wall. The nucleus of the domain wall has energetically favorable sense of magnetization rotation while the two tails have the sense of magnetization rotation that is opposite with respect to the nucleus one, making the integral rotation angle to be zero. The reversal of the sense of magnetization rotation implies alternating electric polarization: the electric polarity of the tails is also opposite to that of the nucleus one.

In homogeneous magnetic media under the influence of electric field the 0°-DW state becomes energetically favorable compared to the single domain state provided that the domain wall has a nonzero Néel-component. This case corresponds to the so-called quasi-Bloch domain wall. Another solution is the pure Néel-type domain wall with compensated electric charge integrated over the domain wall width. For the 0°-DW Néel-type domain wall the electric-field gradient is the key requirement for nucleation: the field gradient enables to maximize the electric polarization under the electrode leaving the tails with the opposite electric polarity on the periphery. The 0°-DW Néel-type domain wall can be considered as a transitional state between the homogeneously magnetized state and the electric-field–induced domain observed in experiments [18,19].

* * *

The work is supported by RFBR grant No. 19-02-00828. The authors are grateful to Z. A. Pyatakova for help with figure drawing and Z. V. Gareeva for valuable discussion and help with writing the text. FAM and APP acknowledge the support of RFBR grant No. 19-32-50020.

REFERENCES

[1] Hill N. A., *J. Phys. Chem. B*, **104** (2000) 6694.
[2] Pyatakov A. P. and Zvezdin A. K., *Phys.-Usp.*, **55** (2012) 557.
[3] Fiebig M., Lottermoser T., Meier D. and Trassin M., *Nat. Rev. Mater.*, **1** (2016) 16046.
[4] Catalan G., Béa H., Fusil S., Bibes M., Paruch P., Barthélémy a. and Scott J., *Phys. Rev. Lett.*, **100** (2008) 027602.
[5] Popov A. I., Zvezdin K. A., Gareeva Z. V., Mazhitova F. A., Vakhitov R. M., Yumaguzin A. R. and Zvezdin A. K., *J. Phys.: Condens. Matter*, **28** (2016) 456004.
[6] Karpov P. I. and Mukhin S. I., *Phys. Rev. B*, **95** (2017) 195136.
[7] Pyatakov A. P., *Physica B*, **542** (2018) 59.
[8] Sharma P. and Schoenherr P., *Materials (Basel)* **12** (2019) 2927.
[9] Catalan G., Seidel J., Ramesh R. and Scott J., *Rev. Mod. Phys.*, **84** (2012) 119.
[10] Dzyaloshinskii I., *EPL*, **83** (2008) 67001.
[11] Logginov A. S., Meshkov G. A., Nikolaev A. V., Nikolaeva E. P., Pyatakov A. P. and Zvezdin A. K., *Appl. Phys. Lett.*, **93** (2008) 182510.
[12] Arzamastseva G. V., Balbashov A. M., Lisovskii F. V., Mansvetova E. G., Temiryazev A. G. and Temiryazeva M. P., *J. Exp. Theor. Phys.*, **120** (2015) 687.
[13] Khokhlov N. E., Khramova A. E., Nikolaeva E. P., Kosykh T. B., Nikolaev A. V., Zvezdin A. K., Pyatakov A. P. and Belotelov V. I., *Sci. Rep.*, **7** (2017) 264.
[14] Pyatakov A. P., Sechin D. A., Sergeev A. S., Nikolaev A. V., Nikolaeva E. P., Logginov A. S. and Zvezdin A. K., *EPL*, **93** (2011) 17001.
[15] Veshchunov I. S., Mironov S. V., Magrini W., Stolyarov V. S., Rossolenko A. N., Skidanov V. A., Trebbia J.-B., Buzdin A. I., Tamarat P. and Lounis B., *Phys. Rev. Lett.*, **115** (2015) 027601.
[16] Pyatakov A. P., Belotelov V. I., Kulikova D. P., Khokhlov N. E., Pyatakova Z. A. and Nikolaev A. V., *J. Magn. & Magn. Mater.*, **440** (2017) 60.
[17] Koronovskyy V. E. and Vakyla Y. A., *Physica B*, **547** (2018) 79.
[18] Kulikova D. P., Pyatakov A. P., Nikolaeva E. P., Sergeev A. S., Kosykh T. B. and Pyatakova Z. A., *JETP Lett.*, **104** (2016) 197.
[19] Kulikova D. P., Gareev T. T., Nikolaeva E. P., Kosykh T. B., Nikolaev A. V., Pyatakova Z. A., Zvezdin A. K. and Pyatakov A. P., *Phys. Status Solidi - Rapid Res. Lett.*, **12** (2018) 1800066.
[20] Schott M., Bernand-Mantel A., Ranno L., Pizzini S., Vogel J., Béa H., Baraduc C., Auffret S., Gaudin G. and Givord D., *Nano Lett.*, **17** (2017) 3006.
[21] Srivastava T., Schott M., Juge R., Křižáková V., Belmeguenai M., Roussigné Y., Bernand-Mantel A., Ranno L., Pizzini S., Chérif S. M., Stashkevich A., Auffret S., Boulle O., Gaudin G., Chshiev M., Baraduc C. and Béa H., *Nano Lett.*, **18** (2018) 4871.
[22] Smolenskii I. E. and Chupis G. A., *Sov. Phys. Usp.*, **25** (1982) 475.

[23] Sparavigna A., Strigazzi A. and Zvezdin A., *Phys. Rev. B*, **50** (1994) 2953.

[24] Mostovoy M., *Phys. Rev. Lett.*, **96** (2006) 067601.

[25] Katsura H., Nagaosa N. and Balatsky A. V., *Phys. Rev. Lett.*, **95** (2005) 057205.

[26] Sergienko I. A. and Dagotto E., *Phys. Rev. B*, **73** (2006) 094434.

[27] Bar'yakhtar V. G., L'vov V. A. and Yablonskii D. A., *JETP Lett.*, **37** (1983) 673.

[28] Sosnowska I. and Zvezdin A. K., *J. Magn. & Magn. Mater.*, **144** (1995) 167.

[29] Cheong S.-W. and Mostovoy M., *Nat. Mater.*, **6** (2007) 13.

[30] Pamyatnykh L. A., Kandaurova G. S., Shamsutdinov M. A., Plavski V. V. and Filippov B. N., *J. Magn. & Magn. Mater.*, **234** (2001) 469.

[31] Borisov A. B., Kiseliev V. V. and Talutz G. G., *Solid State Commun.*, **44** (1982) 411.

[32] Vakhitov R. M. and Yumaguzin A. R., *Phys. Solid State*, **43** (2001) 65.

[33] Vakhitov R. M. and Magadeev E. B., *Phys. Met. Metallogr.*, **115** (2014) 849.

[34] Sapozhnikov V. M., *J. Magn. & Magn. Mater.*, **396** (2015) 338.

[35] Vakhitov R. M., Akhmetova A. A. and Solonetskii V. R., *Phys. Solid State*, **61** (2019) 319.

[36] Bogdanov A. and Hubert A., *J. Magn. & Magn. Mater.*, **138** (1994) 255.

[37] Mühlbauer S., Binz B., Jonietz F., Pfleiderer C., Rosch A., Neubauer A., Georgii R. and Böni P., *Science*, **323** (2009) 915.

[38] Zvezdin A. K. and Pyatakov A. P., *EPL*, **99** (2012) 57003.